



IMPACT PROPERTIES OF CFRP/AL HYBRID BEAM FOR ABSORBING IMPACT ENERGY IN SIDE COLLISION OF AUTOMOBILES

Goichi Ben*, Yoshio Aoki**, Nao Sugimoto*

*Nihon University, College of Industrial Technology

**Nihon University, College of Science and Technology

Keywords: CFRP/Al, Hybrid beam, Impact test, F.E.M. Side collision, Automobile

Abstract

Carbon fiber reinforced plastic (CFRP) laminates are used in various industrial fields because they have excellent properties in the specific strength and specific stiffness. The CFRP has a potential of weight reduction in the automotive structure which can contribute to the improvement of mileage as well as the reduction of carbon dioxide. On the other hand, the safety issue in case of collision should be also clarified when employing the CFRP as automotive structures.

In this paper, hybrid beams which consisted of the Al Alloy beam and the CFRP laminate were examined by both experiments and numerical analyses as candidates to replace the conventional steel door guarder beam used inside the automotive door. The experimental relations of impact loading to the displacement for the Al guarder beams with different thicknesses, widths and types of CFRP showed good agreement with those from numerical results. These results show that the numerical method developed here is useful for estimating the impact behavior of CFRP/Al hybrid beams

1. Introduction

It is well known that CO₂ emitted from passenger vehicles is one of major causes of global warming. The most effective method to reduce CO₂ is to produce fuel efficient automobiles. Improvement of the automobile fuel efficiency can be realized by reducing the automobile weight using a lightweight material such as composite materials. Carbon fiber reinforced plastics (CFRP) have been widely used in aerospace industries, industrial goods and other application fields because of their high specific

strength and high specific modulus compared with conventional metals. This means that the CFRP can contribute to lightening the weight of automobiles significantly.

Besides reducing the weight, the safety of automobiles is also a very important issue which needs to be investigated along with the reduction of weight. Collision safety of the automobile has been evaluated by full flap frontal crash, offset frontal crash and side impact tests. In the frontal crash test, it is possible to absorb the energy by largely deforming the front and the rear parts of automobiles. With increasing interests in reducing the automobile weight and securing the safety of passengers, extensive research has been performed in the recent years for collision impact [1-6].

However, in the side impact test, it is hard to absorb the impact energy the same way as the frontal crash, because the survival space of passengers is very narrow. At present, door guarder beams made of steel are used inside the door for absorbing impact energy and their deformation is limited to about 150mm as shown in Fig.1.

In this study, we developed CFRP/Al hybrid beams as impact energy absorption members for side collision as shown in Fig.2. Such members have the advantages of plastic deformation of aluminum alloy combined with high strength and lightweight of CFRP (Fig.3). By using the hybrid beam of aluminum alloy with the CFRP laminate, excellent energy absorption is expected within the limited deformation of 150mm.

The goal of this study is to develop simulation technology for the impact behavior of such hybrid members and to design optimally them.



Fig.1 Door guard beam for side collision

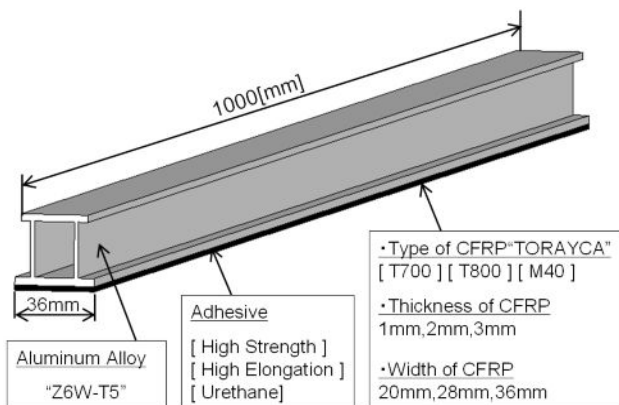


Fig.2 CFRP/Al hybrid beam

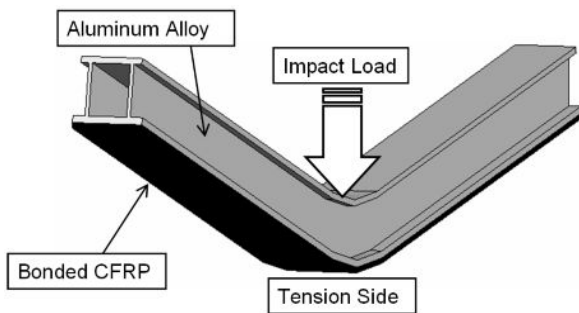


Fig.3 Bending deformation of hybrid beam

2 Experiments

2.1 Specimens of the hybrid beam

An increase of impact energy absorption of Al beam with the CFRP laminate was examined by our past paper [7]. When the thickness of CFRP laminate increase, the impact energy also increased as shown in Fig.4. The hybrid beam with 2.5mm CFRP laminate

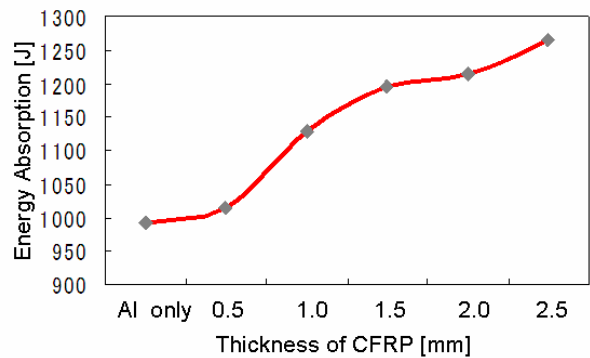


Fig.4 Increase of impact energy absorption

absorbed 25% larger impact energy than that of the Al beam alone.

The specimens of hybrid beams used in this study were different from the former one. The type of Aluminum alloy beam was 7000 series (Z6w-T5) and it has Young's modulus of 70GPa, yield stress of 445GPa, strength of 480MPa and its cross section shape was the unsymmetrical section to the horizontal axis as shown in Fig.21. Three kinds of unidirectional CFRP laminate (T700, M40 and T800) and three types of adhesive (Urethane, High-strength and High-elongation) were used, respectively. Furthermore, the differences of CFRP laminate width (20, 28 and 36mm) and the thickness (1, 2 and 3mm) were also employed. The effects of these design parameters on the impact energy absorption were examined.

2.2 Experimental method

The 1,000 mm length of hybrid beam was supported by two supporters having a head radius of 15mm and the span between the two supporters was 800 mm. In order to evaluate the capacity of crash energy absorption, a larger size of drop tower facility for the impact test was constructed. The beam received an impact load generated by a free drop mass of 100 kg at an impact speed of 55 km/h. The shape of the impactor was a half cylinder having a 100 mm radius and a 200 mm width and the hybrid beam was fixed by belts to prevent from scattering (Fig.5)

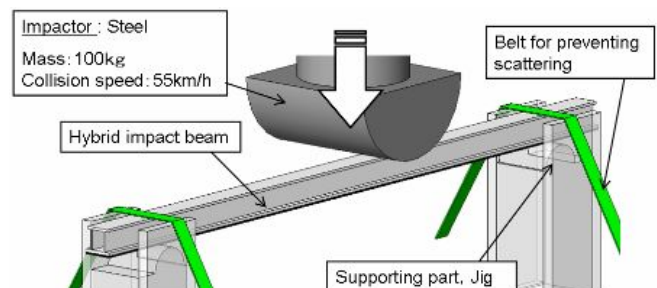


Fig.5 Outline of impact test

The impact load and the displacement of the impactor were measured by load cells attached to both supporters and by a high-speed camera, respectively.

2.3 Results of experiments

18 specimens with combining the design parameters were fabricated and tested. Their specifications are listed in Table 1. Among all the specimens, No.18 specimen absorbed the largest impact energy is shown in Fig.6. The design parameters of this specimen were high elongation adhesive, the thickness of 3mm and width of 36mm of T800 CFRP, respectively. The absorbed impact energy until the displacement of 150mm was 1827J. This value was somewhat higher or almost same as that of the steel door guarder beam. After the impact load reached to the maximum value of 24.0kN at the earlier time of impact, it soon recovered to the almost same value because of the effects of CFRP reinforcement. The center of unidirectional CFRP laminate broke at the displacement of 126 mm and the impact load became to zero at the displacement of 164mm. Fig.7 shows the fiber broke mode of CFRP.

On the other hand, Fig.8 shows the impact test results of No.12 specimen. This specimen could not absorb the larger impact energy and its value was 1493J. This reason was that the CFRP laminate came off the surface of Al beam because the breakage of adhesive was faster than that of CFRP laminate. Fig. 9 shows the breakage of adhesive and CFRP laminate delaminated from the Al beam.

Table1 Combination of the design parameters

No.	CFRP	Thickness [mm]	Width [mm]	Adhesive
1	T700	1	36	Urethane
2	T700	2	28	High Elongation
3	T700	3	20	High Strength
4	M40	1	28	High Elongation
5	M40	2	36	High Strength
6	M40	3	36	Urethane
7	T800	1	36	High Strength
8	T800	2	28	Urethane
9	T800	3	20	High Elongation
10	T700	1	20	High Elongation
11	T700	2	36	High Strength
12	T700	3	28	Urethane
13	M40	1	20	Urethane
14	M40	2	36	High Elongation
15	M40	3	28	High Strength
16	T800	1	28	High Strength
17	T800	2	20	Urethane
18	T800	3	36	High Elongation

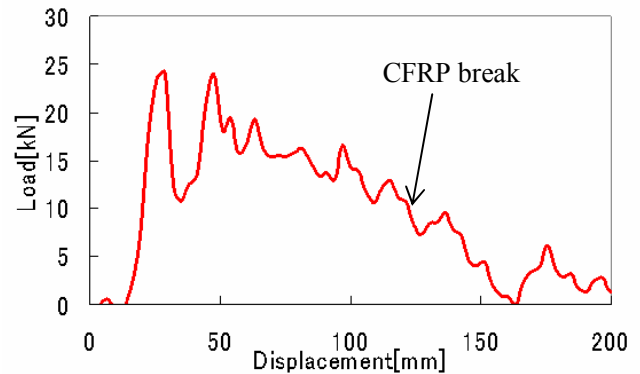


Fig.6 Displacement-load curve of No.18 specimen

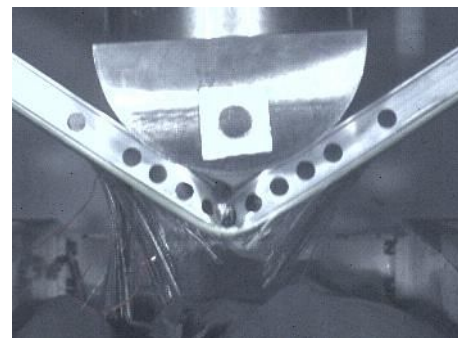


Fig.7 Break of CFRP laminates (Specimen No. 18)

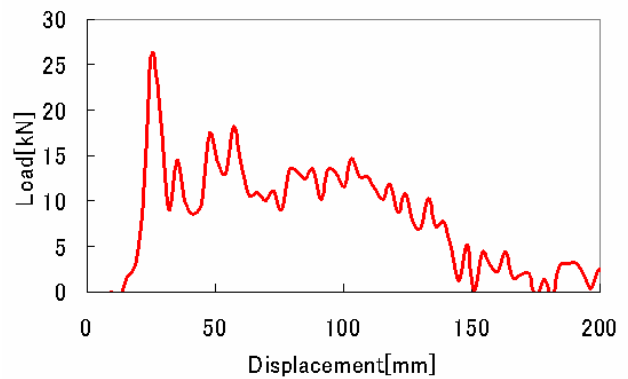


Fig.8 Displacement-load curve of No. 12 specimen



Fig.9 Breakage of Adhesive laminates (Specimen No.12)

3. Impact response analysis by F.E.M.

3.1 Analytical model

In the numerical analysis, a dynamic explicit FEM solver (PAM-CRASH Solver2006) was employed. The analysis model was created based on the size of the specimens, impactor and the support parts in the test. The analysis model is shown in Fig.10. The elastic-plastic shell element (MAT103) for the Al beam part and the unidirectional composite global ply shell element (MAT131, ITYP=1) for the CFRP laminate were used, respectively. The impactor and the supporters were modeled as a rigid body. The mass of 100kg and an initial velocity of 55km/h was given to the impactor. The total node number was 21,583 and the total element number was 19,504.

The contact element between the impactor and the upper surface of hybrid CFRP/Al beam and between the supporter and the lower surface of hybrid CFRP/Al beam was Contact Type 33 with the friction and penalty coefficients of 0.17 and of 0.1, respectively. For the interface of Al beam and the CFRP laminate, “Link Material 303” was used for modeling adhesion of interface.

Table 2 shows the material properties of the aluminum alloy and Fig.11 shows its true strain-true stress curve. Table 3 shows the material properties of three kinds of Adhesive and Table 4 shows the material properties of three kinds of CFRP.

For the failure criterion of Al beam element, a 5% decrease of thickness in the tension state or an increase 30% of thickness in the compression state was used. Next, the failure criteria of adhesive and CFRP laminate were employed “Fracture energy of mode 1 and mode 2 of Link Material 303” and the maximum stress theory, respectively. When the value of the element was over these criteria, it was deleted in the succeeding FEM calculation.

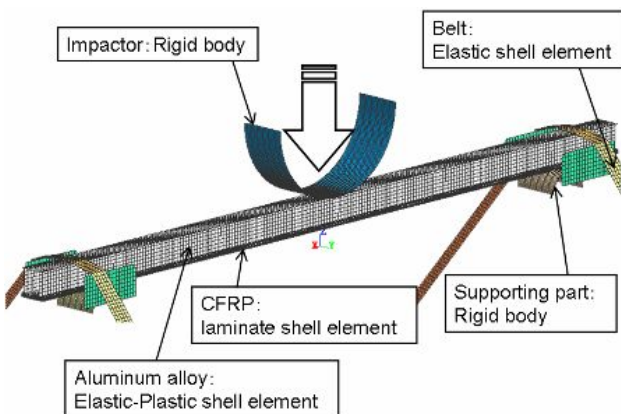


Fig.10 F.E.M. Analytical Model

Table2 Material properties of aluminum alloy

Aluminium Alloy (Z6W-T5)		
Tensile Strength	Elastic Modulus	Plastic Modulus
0.48[GPa]	70[GPa]	10[GPa]

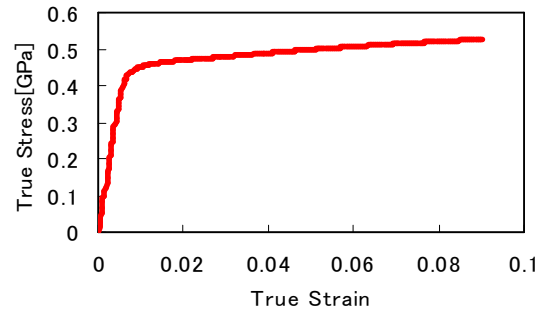


Fig.11 True Strain-True stress curve of aluminum alloy

Table3 Material properties of adhesive

Type of Adhesive	Ft [GPa]	Fs [GPa]	E [GPa]	G [GPa]
High Strength	0.030	0.025	3.00	1.150
High Elongation	0.013	0.013	0.36	0.138
Urethane	0.001	0.001	0.00001	0.0000038

Table4 Material properties of CFRP

CFRP	F_L Tension[GPa]	F_L Compression[GPa]	F_T [GPa]	E_L [GPa]	E_L [GPa]
T700	2.55	1.47	0.069	135	8.5
T800	2.84	1.57	0.080	160	7.8
M40	2.45	1.27	0.053	230	7.7

3.2 Comparison of Experimental and FEM results

Fig 12 shows both impact load to displacement curves obtained by the experiment and the FEM for the No. 18 specimen which absorbed the highest impact energy. Both results showed the almost same impact behavior and the absorbed impact energy obtained by the FEM was 1822J and the error of impact energy was 0.27% to the experimental one. Fig.13 compares the failure mode of hybrid beam and two results showed the same breakage of CFRP laminate at the center of hybrid beam.

In order to demonstrate the effectiveness of FEM method developed here for estimating the impact behavior of hybrid CFRP/Al beam, the result of No.12 specimen which showed the breakage of adhesive, not the breakage of CFRP laminate, was compared with that obtained by FEM. Fig 14 expresses a good agreement of the load –displacement relation except the value of initial peak of load and the error of absorbed impact energy was 7% between both results.

Fig. 15 shows the failure mode obtained two results and the CFRP laminate came off the Al beam in both cases because of the breakage of adhesive.

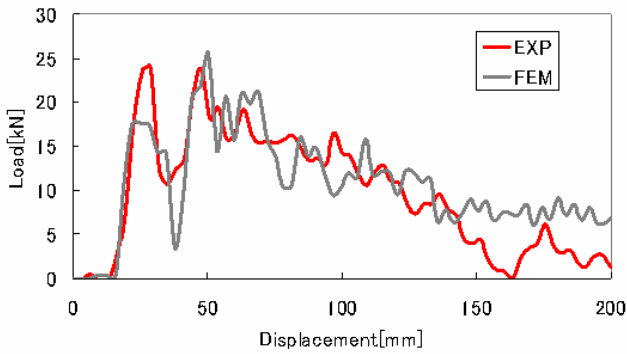


Fig. 12 Comparison of experimental result with F.E.M. one (Specimen No. 18)

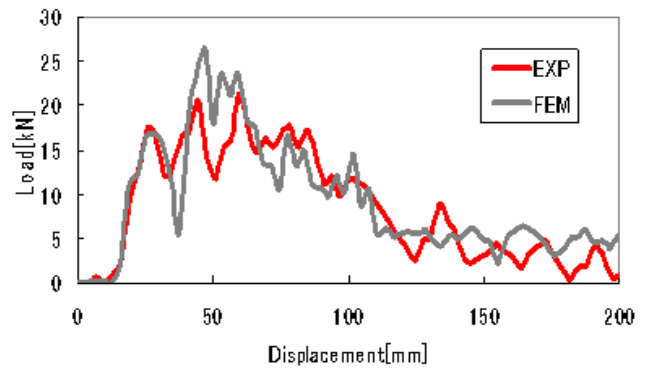


Fig. 16 Comparison of experimental result with F.E.M. one (Specimen No. 11)

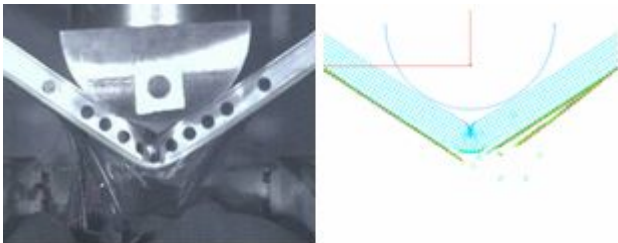


Fig. 13 Comparison of experimental fracture mode with F.E.M. one (Specimen No. 18)

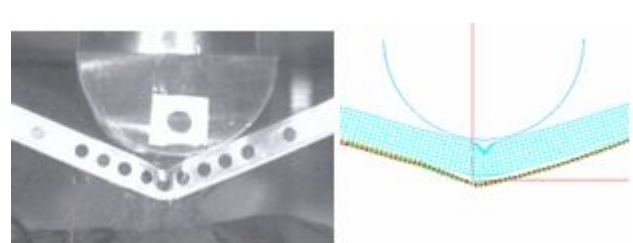


Fig. 17 Comparison of experimental fracture mode with F.E.M. one (Specimen No. 11)

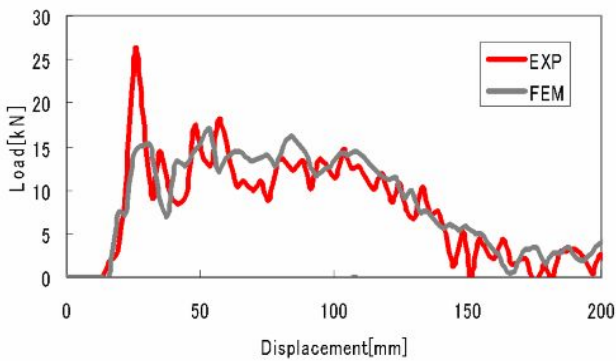


Fig. 14 Comparison of experimental result with F.E.M. one (Specimen No. 12)

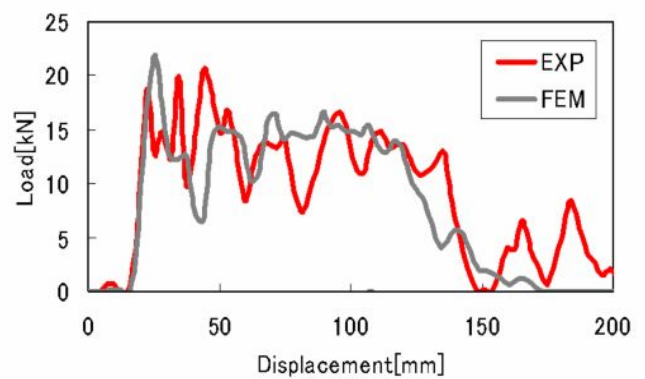


Fig. 18 Comparison of experimental result with F.E.M. one (Specimen No. 17)

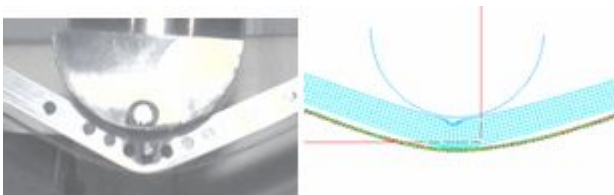


Fig. 15 Comparison of experimental fracture mode with F.E.M. one (Specimen No. 12)

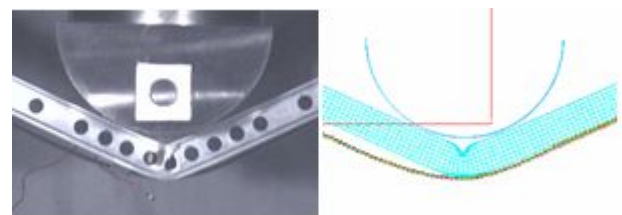


Fig. 19 Comparison of experimental fracture mode with F.E.M. one (Specimen No. 17)

The failure mode of other specimens listed Table 1 showed the mixture of both breakages of CFRP laminate and adhesive. The comparisons of No. 11 and 17 experimental results with those of FEM are shown in Figs. 16, 17 and 18, 19, respectively. They agreed well each others for the load-displacement, the impact energy absorption and the failure mode.

Table 5 lists the impact energy absorption for all of the specimens except No.5 and No. 8 specimens owing to the miss of experiment The specimen No.18 which absorbed the largest impact energy, consisted of 3mm thickness and 40mm width of T800 and the high elongation adhesive.

Table5 Impact energy absorption for all specimens

No.	Type of CFRP	Thickness of CFRP [mm]	Width of CFRP [mm]	Type of Adhesive	Absorbing energy of Experiment [J]	Absorbing energy of Analysis [J]	Error [%]
1	T700	1	36	Urethane	1345	1384	2.9
2	T700	2	28	High-elongation	1342	1358	1.2
3	T700	3	20	High-strength	1605	1685	5
4	M40	1	28	High-elongation	1531	1529	0.13
5	M40	2	20	High-strength	—	—	—
6	M40	3	36	Urethane	1583	1574	0.57
7	T800	1	36	High-strength	1626	1737	6.8
8	T800	2	28	Urethane	—	—	—
9	T800	3	20	High-elongation	1371	1470	7.2
10	T700	1	20	High-elongation	1549	1595	3
11	T700	2	36	High-strength	1570	1627	3.6
12	T700	3	28	Urethane	1487	1591	7
13	M40	1	20	Urethane	1322	1430	8.2
14	M40	2	36	High-elongation	1815	1748	3.7
15	M40	3	28	High-strength	1569	1663	6
16	T800	1	28	High-strength	1667	1692	1.5
17	T800	2	20	Urethane	1636	1613	1.4
18	T800	3	36	High-elongation	1827	1822	0.27

4. Optimum design by F.E.M.

In order to obtain the larger impact energy absorption, the design parameters were changed in the numerical simulation of FEM method because of confirming the effectiveness of this method developed here through the comparison of both results. First, the sort of CFRP was examined while remaining other design parameters. Next, the cross section of Al beam was changed under the condition of keeping same area.

4.1 Comparisons of three kinds of CFRP

In the experiment, the No.18 specimen used T800 CFRP absorbed the largest impact energy. However, the specimens having the CFRP laminate of T700 or M40 and the other same design parameters as the No.18 specimen were not fabricated. Therefore, the two hybrid beams having the CFRP laminate of T700 and M40 were calculated by the FEM method

Fig. 20 compares three results of specimens with T800, T700 and M40. The result of T700 showed the highest first peak of impact load and the largest impact energy absorption until the displacement of 150mm. Its value was 1863J and an increase of 41J was obtained than the case of T800.

Although, the largest strength of CFRP is T800 and the largest Young's modulus of E_L is M40 in Table4, the result of T700 was the most proper CFRP among three CFRPs. In the hybrid of CFRP/Al beam, the CFRP was not necessarily required the larger strength nor the larger Young's modulus. The most important properties of CFRP were the proper strength and Young's modulus to be able to follow the deformation of Al beam.

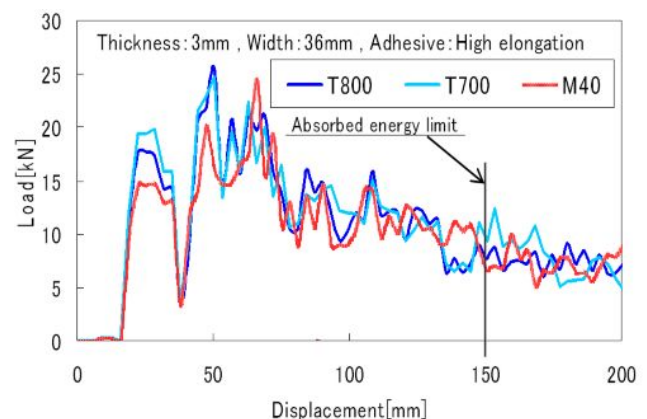


Fig.20 Displacement-load curves of three kinds of hybrid beams with different CFRP.

4.2 Design of Al beam cross-sections

Next the cross section shape of Al beam was change as a design parameter in order to increase the impact energy absorption. Here, the thickness of 3 mm and the width of 36 mm of T700 CFRP and the adhesive of high elongation type were employed in the numerical simulation of FEM. The area of cross section of Al beam used in the experiment (called as the original section) was 366 mm² as shown in Fig. 21 and the four kinds of cross section shape as shown in Figs. 22a-d were devised under the condition of keeping the same area as that of the original beam.

The vertical member of the cross-section in Fig. 22a was increased from 2 to 3 by reducing the thickness of the horizontal members and it was called III section. Fig. 22b shows the higher vertical members compare with those of the original beam aiming larger second moment of area and it called as II section. In Fig. 22c, two vertical members were crossed each other and it was called as X section. Finally, one thicker vertical member was connected to the upper and the lower horizontal members (Fig. 22d) and it was called as I section.

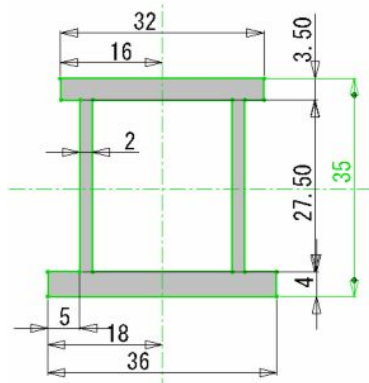


Fig.21 Cross section of original Beam

The displacement-load curves of four hybrid beams having the devised each cross section of Al beam were compared with that of original hybrid beam in Fig.23. Among them, the II section showed the highest impact load at the earlier time of impact and the III section presented the larger and constant impact load (about 20kN) until the displacement of 120mm.

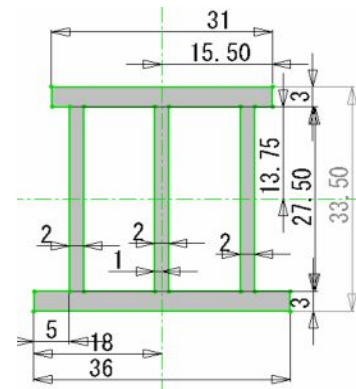


Fig.22a Cross section of III Beam

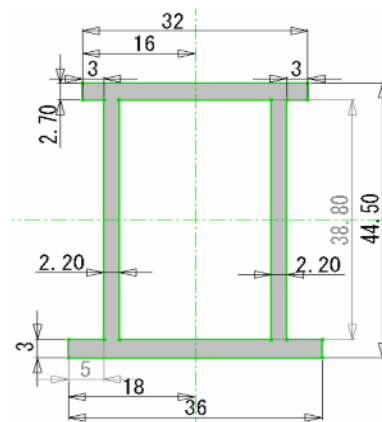


Fig.22b Cross section of II Beam

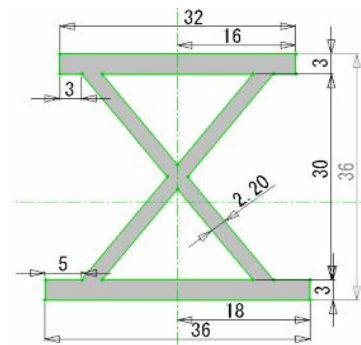


Fig.22c Cross section of X Beam

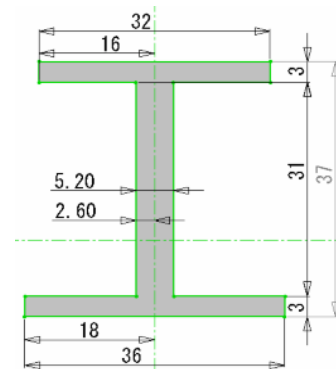


Fig.22d Cross section of I Beam

The impact energies of absorption for the hybrid beams with the III, II and X sections were 2245J, 2171J and 2056J, respectively. They were larger than 1822J of the original hybrid beam except the hybrid beam with the I section. Therefore, the absorbed impact energy of the hybrid beam with the III section was 23% larger than that of the original one.

Fig.24 shows the deformation of hybrid beam with III section and it showed the symmetric mode.

5. Conclusions

1. The CFRP/Al hybrid door guarder beam showed an excellent performance of absorbing impact energy and its maximum displacement after the impact was smaller than that of steel one.
2. The CFRP/Al hybrid beam with the thicker CFRP showed the larger impact failure displacement of hybrid beam because its fracture was extended by the thicker CFRP and then it absorbed more impact energy.
3. From the comparison of FEM results with the experimental ones for specimens of CFRP/Al hybrid beams, the proposed numerical method was found to be very useful for analyzing the hybrid beams.
4. The change of cross section of Al beam increased the impact energy absorption by the numerical simulation. Therefore, changing the design parameters of the hybrid beam may result in further increase of impact energy absorption.

This study was conducted as part of a Japanese National Project R&D of Carbon Fiber-Reinforced Composite Materials to Reduce Automobile Weight supported by NEDO (the New Energy and Industrial Technology Development Organization) and the authors acknowledge the assistance of Toray Industries, Inc. who supplied the materials for these test specimens.

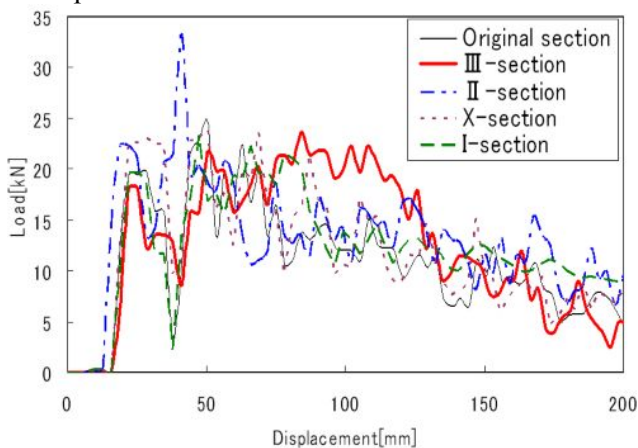


Fig.23 Comparisons of displacement-load curves for five hybrid beams

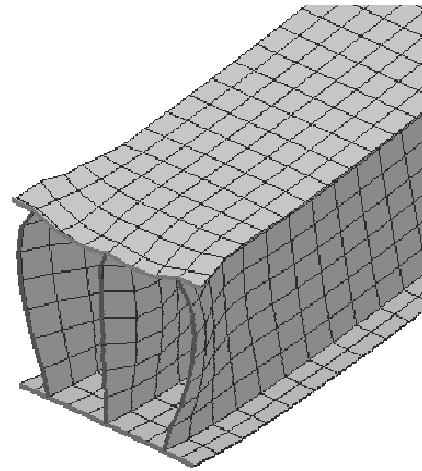


Fig.24 Deformation of hybrid beam with III section after impact

References

1. P.K. Mallick and L.J. Broutman, J. Testing and Evaluation, 5, 190 (1977)
2. S.S. Cheon, T.S. Lim and D.G. Lee, Comp Struct, 46, 267 (1999)
3. D.G. Lee, T.S. Lim and S.S. Cheon, Comp Struct, 50, 381 (2000)
4. G. Ben, T. Uzawa, H.S. Kim, Y. Aoki, H. Mitsuishi and A. Kitano, Transaction of JSME Series A, 70(694), 824 (2004) (in Japanese)
5. A. G. Caliska, Proceedings of IME2002, ASME, International Mechanical Engineering Congress & Exposition(2002)
6. H.S. Kim, G. Ben and Y. Iizuka, Proceedings of 11th Japan-US Conference of Composite Materials (2004)
7. G. Ben, Y. Aoki and H.S. Kim, Proceedings of 12th US-Japan Conference on Composite Materials (2006).